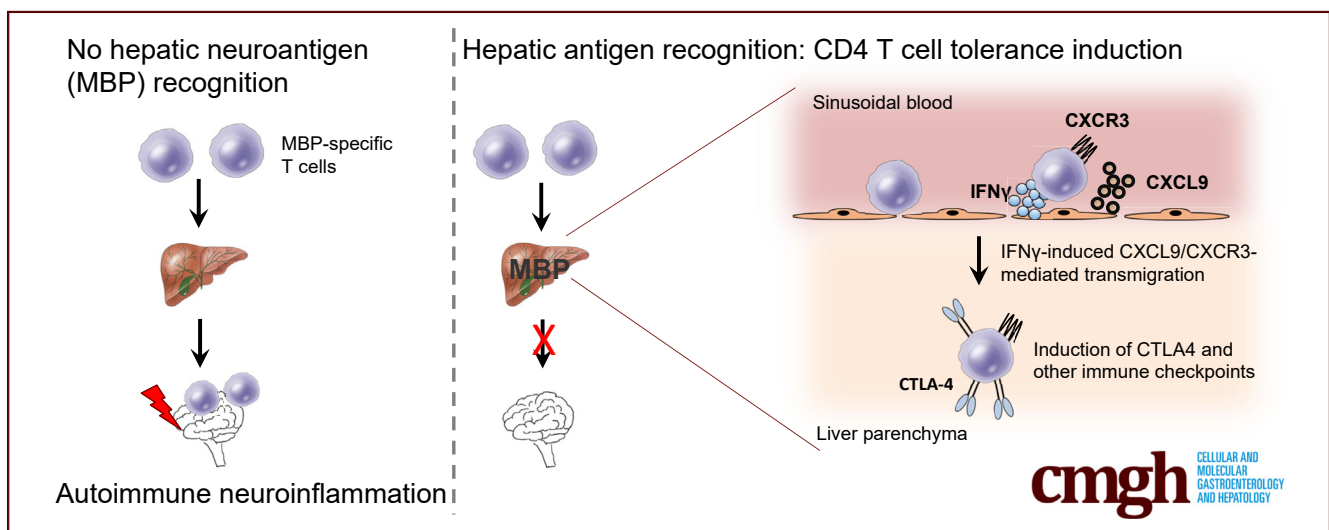


## ORIGINAL RESEARCH

IFN $\gamma$  and CTLA-4 Drive Hepatic CD4 T-Cell Tolerance and Protection From Autoimmunity in Mice

Daria Krzikalla,<sup>1</sup> Alena Laschtowitz,<sup>1</sup> Lisa Leyoldt,<sup>1</sup> Cornelia Gottwick,<sup>1</sup> Pia Averhoff,<sup>1</sup> Sören Weidemann,<sup>2</sup> Ansgar W. Lohse,<sup>1,3</sup> Samuel Huber,<sup>1,3</sup> Christoph Schramm,<sup>1,3,4</sup> Dorothee Schwinge,<sup>1,3</sup> Johannes Herkel,<sup>1,3,§</sup> and Antonella Carambia<sup>1,3,§</sup>

<sup>1</sup>Department of Medicine I, University Medical Center Hamburg-Eppendorf, Hamburg, Germany; <sup>2</sup>Department of Pathology, University Medical Center Hamburg-Eppendorf, Hamburg, Germany; <sup>3</sup>Hamburg Center for Translational Immunology, University Medical Center Hamburg-Eppendorf, Hamburg, Germany; and <sup>4</sup>Martin Zeitz Center for Rare Diseases, University Medical Center Hamburg-Eppendorf, Hamburg, Germany



## SUMMARY

In this study, we show that interferon  $\gamma$  and cytotoxic T-lymphocyte-associated protein 4 are essential for induction of antigen-specific CD4 T-cell tolerance in the liver and prevention of autoimmune disease. Therefore, this pathway represents a potential treatment target to regulate hepatic immune responses.

**BACKGROUND & AIMS:** The liver has a distinct capacity to induce immune tolerance to hepatic antigens. Although liver tolerance can be advantageous for preventing autoimmune and inflammatory diseases, it also can be detrimental by preventing immune surveillance of infected or malignant cells. Here, we investigated the immune mechanisms that establish hepatic tolerance.

**METHODS:** Tolerance was investigated in C-reactive protein (CRP)-myelin basic protein (MBP) mice expressing the neuroantigen MBP in hepatocytes, providing profound resistance to MBP-induced neuroinflammation. Tolerance induction was studied after transfer of MBP-specific CD4 T cells into

CRP-MBP mice, and tolerance mechanisms were tested using depleting or blocking antibodies.

**RESULTS:** Although tolerant CRP-MBP mice display increased numbers of forkhead box P3+ regulatory T cells, we here found them not essential for the maintenance of hepatic tolerance. Instead, upon MBP recognition in the liver, MBP-specific T cells became activated to produce interferon (IFN) $\gamma$ , which, in turn, induced local up-regulation of recruitment molecules, including Chemokine (C-X-C motif) ligand9 and its receptor C-X-C motif chemokine receptor3, facilitating endothelial translocation and redirection of MBP-specific T cells into the hepatic parenchyma. There, the translocated MBP-specific CD4 T cells partly converted into interleukin 10-producing type 1 regulatory T cells, and significantly up-regulated the expression of immune checkpoint molecules, notably cytotoxic T-lymphocyte-associated protein 4 (CTLA-4). Intriguingly, although liver tolerance was not affected by impairment of interleukin 10 signaling, concomitant blockade of IFN $\gamma$  and CTLA-4 abrogated hepatic tolerance induction to MBP, resulting in neuroinflammatory autoimmune disease in these mice.

**CONCLUSIONS:** IFN $\gamma$ -mediated redirection of autoreactive CD4 T cells into the liver and up-regulation of checkpoint molecules,

including CTLA-4, were essential for tolerance induction in the liver, hence representing a potential treatment target for boosting or preventing liver tolerance. (*Cell Mol Gastroenterol Hepatol* 2024;17:79–91; <https://doi.org/10.1016/j.jcmgh.2023.09.006>)

**Keywords:** Hepatic Tolerance; Regulatory T Cells; Immune Checkpoints; Co-inhibition.

The liver has a distinct capacity to induce immune tolerance,<sup>1,2</sup> indicated by its ability to suppress pathogenic immunity to gut-derived antigens,<sup>3</sup> or rejection of allografts.<sup>4,5</sup> Importantly, the tolerogenic capacity of the liver can be harnessed for the treatment of autoimmune diseases that affect extrahepatic tissues. Indeed, we previously have shown that ectopic expression of a neuroantigen in the liver, which was facilitated by gene transfer to hepatocytes, provided antigen-specific protection from autoimmune neuroinflammation.<sup>6</sup> Moreover, antigen-specific protection from autoimmune disease also could be achieved by selective delivery of autoantigen peptides to tolerogenic antigen-presenting cells in the liver, such as liver sinusoidal endothelial cells or Kupffer cells, using liver-targeting nanoparticles.<sup>7–9</sup>

It is likely that the liver has evolved the capacity for tolerance induction to prevent tissue-damaging inflammation in response to a multitude of hepatic neoantigens derived from food and metabolism. Thus, antigen-specific tolerance induction in the liver is advantageous because it can prevent liver damage and autoimmune disease; however, hepatic tolerance comes at the expense of an increased risk for chronic infections or cancer because hepatic tolerance also can prevent effective elimination of infected<sup>10</sup> or malignant cells.<sup>11</sup> To develop effective therapies for these different conditions, it will be important to better understand the immune mechanisms leading to hepatic tolerance. The tolerance-inducing potential of the liver most likely is owing to its unique microenvironment made of several tolerogenic antigen-presenting cell types, which can interact effectively with circulating T cells under the rather slow blood flow in the liver sinusoids.<sup>1,2</sup> These interactions have been shown to confer inhibitory effects on CD8 and CD4 T cells,<sup>12–14</sup> or to facilitate the induction of CD4+ forkhead box P3 (FOXP3)+ regulatory T cells (Tregs) by conversion from conventional effector CD4 T cells.<sup>6,15</sup> Moreover, it has been reported that another type of regulatory T cell, the interleukin (IL)10-producing type 1 regulatory T cells (Tr1) cells,<sup>16</sup> which do not express FOXP3, can be generated in the liver and suppress inflammation.<sup>17,18</sup>

Here, we aimed to elucidate the immune mechanisms behind antigen-specific tolerance induced in the liver. To that end, we used the transgenic C-reactive protein (CRP)-myelin basic protein (MBP) mouse model in which hepatic autoantigen presentation was facilitated by gene transfer of the autoantigen MBP to hepatocytes.<sup>6</sup> In these mice, MBP-specific CD4 T cells can recognize their cognate autoantigen both in the liver and in the central nervous system (CNS); nonetheless, these mice are robustly resistant to

induction of autoimmune neuroinflammation. We previously have shown that FOXP3+ Tregs are important for tolerance induction in this model because adoptive transfer of Tregs from CRP-MBP mice could protect wild-type recipients from autoimmune disease,<sup>6</sup> and protected CRP-MBP mice featured increased Treg frequencies.<sup>15</sup> Yet, surprisingly, we found here that in vivo impairment of FOXP3+ Tregs in CRP-MBP mice did not break established hepatic tolerance. Likewise, blockade of IL10 signaling, which is important for Tr1 cells, did not precipitate autoimmune disease. Instead, protection from autoimmunity was critically dependent on the interferon  $\gamma$  (IFN $\gamma$ )-mediated redirection of antigen-specific T cells into the liver followed by induction of immune checkpoint molecules, including cytotoxic T-lymphocyte-associated protein 4 (CTLA-4).


## Results

### *Treg/T-effector Imbalance Does Not Cause Autoimmune Disease in CRP-MBP Mice*

We previously have shown that tolerance induction induced by ectopic expression of MBP in the liver protects mice from autoimmune CNS pathology, which was dependent at least in part on the peripheral generation of FOXP3+CD25+ Tregs.<sup>6</sup> Here, we explored whether classic FOXP3+ Tregs were essential for maintenance of hepatic tolerance, or whether in case of Treg failure, compensatory mechanisms might safeguard hepatic tolerance. To that end, we depleted Tregs from MBP-immunized tolerant CRP-MBP mice using the Treg-depleting antibody PC61. This treatment resulted in a significant reduction of Treg frequencies in the spleens to an average of 1.64% CD4+CD25+FOXP3+ Tregs, as compared with 11.8% CD4+CD25+FOXP3+ Tregs in isotype antibody-treated control mice (**Figure 1A**). A similar reduction to an average of 2.48% CD4+CD25+FOXP3+ Tregs also were found in the livers, as compared with 9.75% CD4+CD25+FOXP3+ Tregs in isotype-treated control mice (**Figure 1B**). However, despite significantly reduced Treg numbers upon anti-CD25 antibody treatment, CRP-MBP mice did not develop autoimmune pathology in the CNS upon immunization to MBP, in

<sup>§</sup>Authors share co-senior authorship.

**Abbreviations used in this paper:** CNS, central nervous system; CRP, C-reactive protein; CTLA-4, cytotoxic T-lymphocyte-associated protein 4; CXCL, Chemokine (C-X-C motif) ligand; CXCR, CXC motif chemokine receptor; dnIL10R, dominant-negative IL10 receptor; EAE, experimental autoimmune encephalomyelitis; eGFP, enhanced green fluorescent protein; FOXP3, forkhead box P3; HBV, hepatitis B virus; IFN $\gamma$ , interferon  $\gamma$ ; IL, interleukin; MBP, myelin basic protein; NPC, nonparenchymal cell; PBS, phosphate-buffered saline; PD-1, programmed cell death 1; qPCR, quantitative polymerase chain reaction; TIGIT, T-cell immunoreceptor with Ig and immunoreceptor tyrosine-based inhibitory motif (ITIM) domains; TIM3, T-cell immunoglobulin and mucin domain-containing protein 3; Tr1, type 1 regulatory T cell; Treg, regulatory T cell; WT, wild-type.

 Most current article

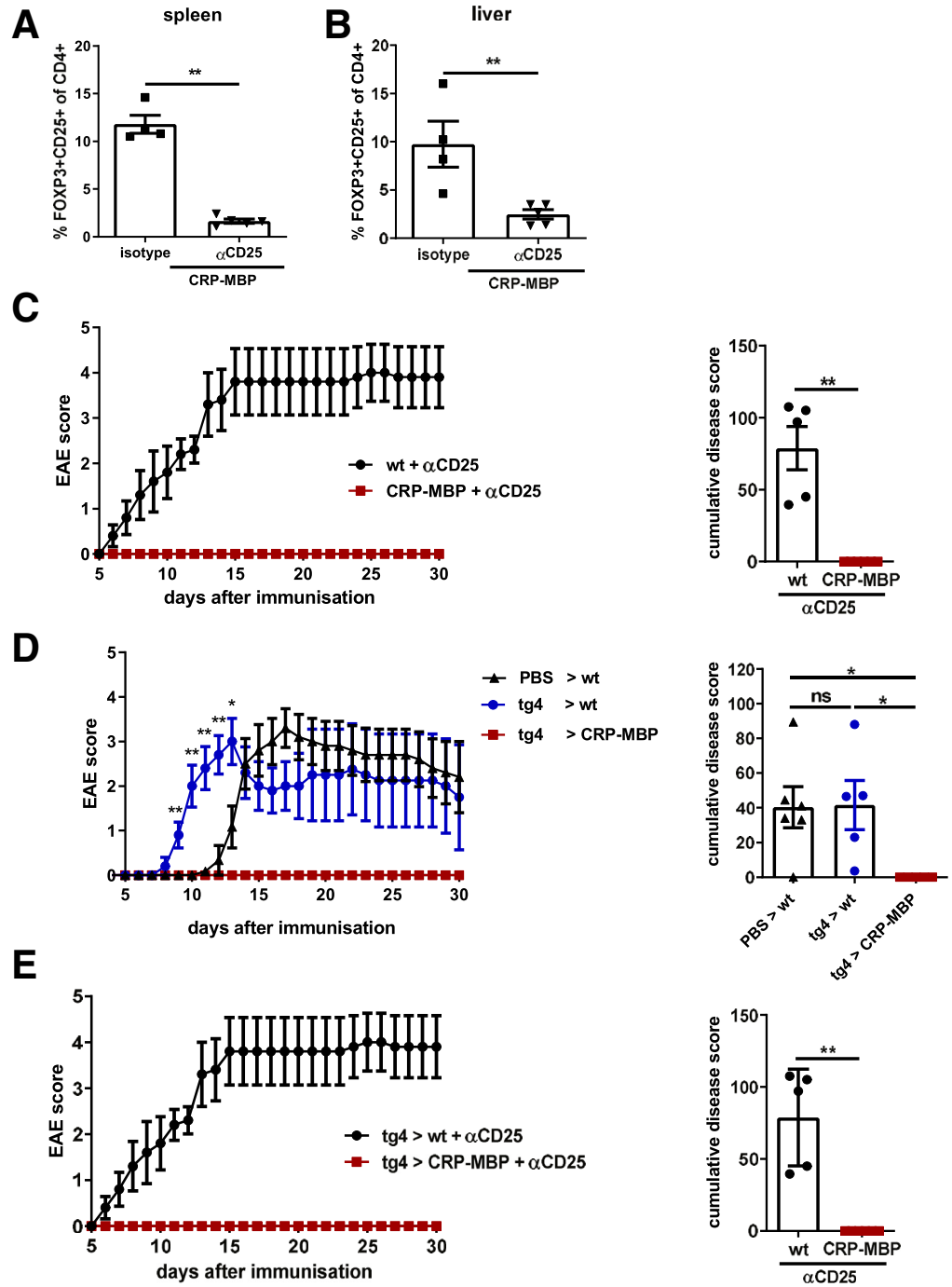
© 2023 The Authors. Published by Elsevier Inc. on behalf of the AGA Institute. This is an open access article under the CC BY-NC-ND license (<http://creativecommons.org/licenses/by-nc-nd/4.0/>).

2352-345X

<https://doi.org/10.1016/j.jcmgh.2023.09.006>

### Figure 1. Impairment of regulatory T cells does not precipitate autoimmune disease in CRP-MBP mice.

CRP-MBP mice or littermate controls (WT) were immunized to MBP and replenished with MBP-specific CD4 T cells 1 day later. (A and B) CRP-MBP mice were treated with anti-CD25 monoclonal antibody PC61.5.3 or isotype control antibody twice a week. Frequency of FOXP3+CD25+ T cells was determined on day 7 after immunization, as compared with isotype control-treated mice in (A) spleen and (B) liver. (C) EAE course and cumulative disease score in Treg-depleted WT and CRP-MBP mice. (D) EAE course and cumulative disease score in WT or CRP-MBP mice after transfer of pathogenic tg4 T cells, as compared with PBS-treated WT mice. (E) tg4 T cells were transferred to Treg-depleted WT or CRP-MBP recipients and EAE development was assessed. Data are shown as means  $\pm$  SD,  $n = 4-6$  per group. Data of 1 independent experiment out of multiple similar experiments are shown. Statistical analysis was performed using the Mann-Whitney  $U$  test for comparison of 2 groups. For multiple comparisons, the Kruskal-Wallis test and the Dunn multiple comparison test were applied. \* $P < .05$ , \*\* $P < .01$ .



contrast to nontransgenic control mice treated with anti-CD25 antibody (Figure 1C). To further minimize the ratio of CD4+CD25+FOXP3+ Tregs to MBP-specific CD4 T-effector cells in these mice, we concomitantly depleted Tregs and transferred an excess of MBP-specific CD4 T cells from T-cell-receptor transgenic tg4 mice.<sup>19</sup> Specifically,  $5 \times 10^6$  MBP-specific CD4 T cells from naïve tg4 mice were transferred into CRP-MBP recipient mice that expressed MBP in the liver, or into littermate controls without hepatic MBP expression (wild type [WT]). The recipient mice then were immunized to MBP to induce activation of the

transferred autoreactive CD4 T cells in the draining lymph nodes and autoimmune neuroinflammation. As expected, WT mice receiving tg4 cells developed accelerated experimental autoimmune encephalomyelitis (EAE), as compared with WT mice receiving phosphate-buffered saline (PBS) (Figure 1D). However, when MBP-specific CD4 T cells (tg4) were transferred into CRP-MBP mice, these mice remained completely protected from autoimmune neuroinflammation. When concomitantly performing Treg depletion and adoptive transfer of MBP-specific CD4 T-effector cells, hepatic MBP tolerance was nonetheless maintained in

CRP-MBP mice (Figure 1E). Thus, Treg depletion was not sufficient to break established tolerance in CRP-MBP mice, even in excess of MBP-reactive effector T cells. These findings indicated that Treg-independent mechanisms could compensate for the loss of Treg and maintain hepatic tolerance in these mice.

### *IL10 Signaling Is Not Required for Maintenance of Hepatic Tolerance in CRP-MBP Mice*

It was possible that FOXP3<sup>+</sup> Treg impairment in CRP-MBP transgenic mice could be compensated for by Tr1 cells, which might prevent autoimmune pathology. Indeed, we noted that the transferred tg4 T cells in the livers of MBP-expressing CRP-MBP mice had a greatly increased proportion of cells co-expressing LAG3 and CD49b, as compared with tg4 T cells retrieved from control mice lacking MBP in the liver (Figure 2A). Co-expression of LAG3 and CD49b has been described to enrich IL10-producing FOXP3-negative Tr1 cells.<sup>20</sup> To clarify whether the LAG3/CD49b co-expressing cells in the liver of CRP-MBP mice were indeed bona fide Tr1 cells,<sup>21</sup> we assessed their capabilities to produce IL10. To that end, we transferred modified tg4 T cells, which carried an IL10<sup>enhanced green fluorescent protein(eGFP)</sup> reporter construct,<sup>22</sup> into MBP-immunized CRP-MBP mice. We then retrieved the transferred cells from the livers after 6 days and analyzed for LAG3/CD49b co-expression and IL10eGFP reporter activity. We found that a fraction of 13% (on average) of the LAG3/CD49b co-expressing cells showed IL10<sup>eGFP</sup> reporter activity in CRP-MBP mice, as compared with 4% in littermate controls (Figure 2B). Accordingly, 1.5% of the transferred tg4 cells were converted into IL10+LAG3+CD49b+ Tr1 cells in livers of CRP-MBP mice, whereas only 0.1% of tg4 T cells retrieved from livers of littermate controls displayed a Tr1 phenotype. Hence, there was a 15-fold induction of Tr1 cells in CRP-MBP mice compared with controls (Figure 2C). Although their cell numbers were low, the induced Tr1 cells nonetheless might be relevant for maintenance of hepatic tolerance to MBP.

Because it is difficult to deplete Tr1 cells in vivo, we thus targeted IL10 instead, which is considered to represent the prime regulatory mechanism of these cells.<sup>16</sup> To that end, we administered an antibody to the IL10 receptor that inhibits IL10 signaling.<sup>23</sup> Nonetheless, inhibition of IL10 signaling did not precipitate disease symptoms in CRP-MBP transgenic mice, indicating that IL10 signaling was not essential for tolerance (Figure 2D). To confirm these findings, we used CRP-MBP tg4 dominant-negative IL10 receptor (dnIL10R) mice, which have IL10-insensitive T cells owing to expression of a dominant-negative IL10 receptor.<sup>24</sup> In addition, to achieve a combined impairment of both IL10 signaling and FOXP3<sup>+</sup> Tregs, we depleted FOXP3<sup>+</sup> Tregs in CRP-MBP tg4 dnIL10R mice in vivo using the Treg-depleting antibody PC61,<sup>25</sup> and immunized to MBP. Despite this treatment, these mice did not show EAE symptoms (Figure 2E). These findings indicated that even a combined impairment of FOXP3<sup>+</sup> Tregs and IL10 signaling did not precipitate autoimmune pathology, when the

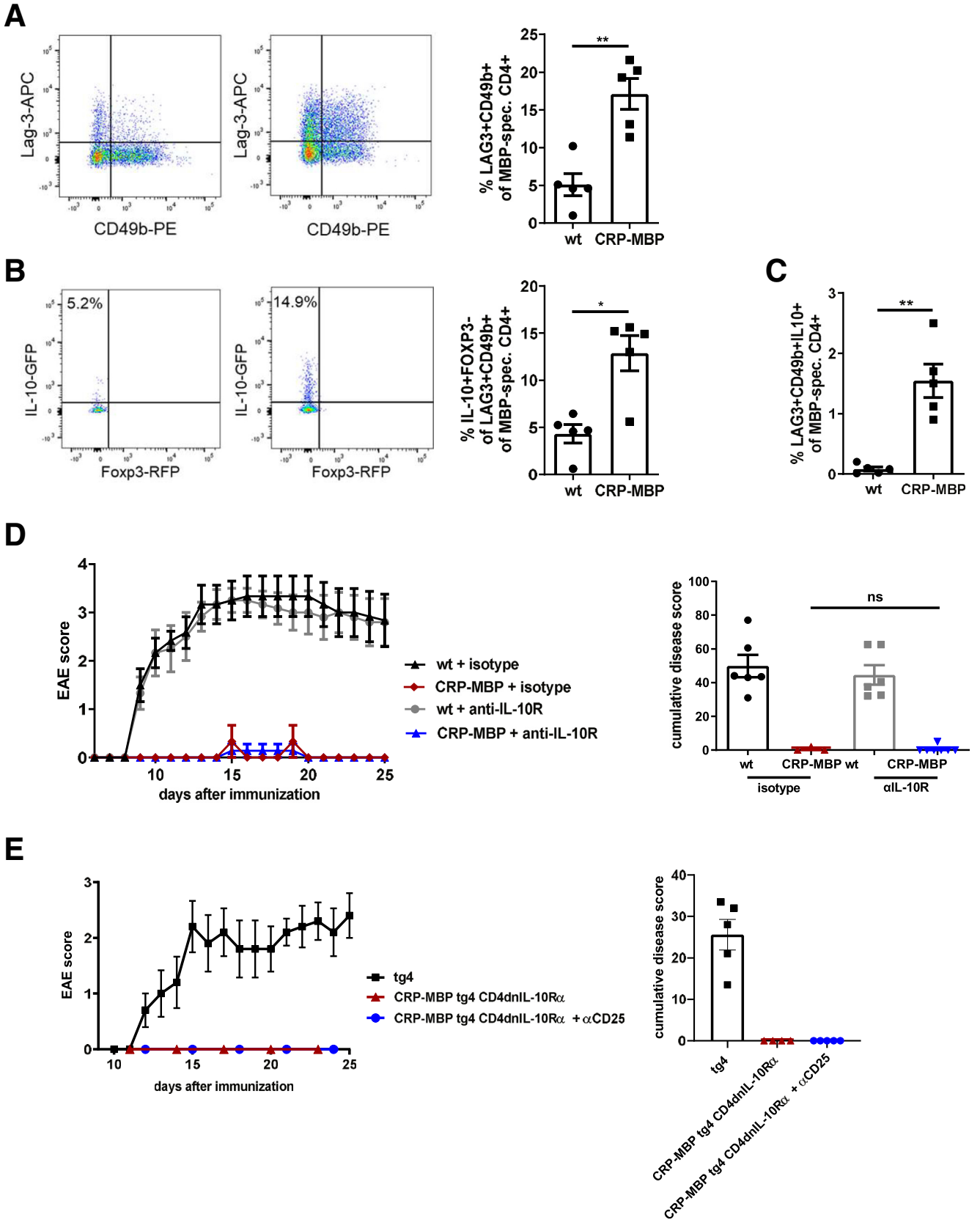
autoantigen MBP was expressed in the liver. Thus, Tregs and IL10 produced by Tr1 cells seemed to be expendable for the maintenance of hepatic immune tolerance in this model.

### *Accumulation of Autoreactive CD4 T Cells in Livers of MBP-Transgenic Mice*

To further explore the Treg-independent tolerance mechanisms in CRP-MBP transgenic mice, we examined the fate of the transferred MBP-specific effector T cells in CRP-MBP mice or littermate controls. Interestingly, liver histology revealed a pronounced presence of mainly periportal lymphocytic infiltrates, together with few scattered intralobular lymphocyte clusters in CRP-MBP mice on day 6 after tg4 T-cell transfer; in contrast, the littermate control recipients showed a much lower degree of lymphocytic liver infiltration (Figure 3A). Correspondingly, we found significantly increased numbers of transferred autoreactive T cells in the livers of CRP-MBP mice on day 6 after transfer compared with the livers of control recipients (Figure 3B). These findings indicated that circulating MBP-specific T-effector cells had translocated across the sinusoidal endothelium into the liver upon recognition of their cognate antigen in CRP-MBP mice. To confirm this finding, we performed immunohistologic staining of CD4 (red) and CD45.1 (light blue) on liver sections of CRP-MBP mice, showing hepatic infiltration mainly of transferred CD45.1-negative MBP-specific CD4 T cells, but also some endogenous CD45.1-positive cells (Figure 3C). Regarding the autoreactive T-cell response in the liver, we found significantly increased IFN $\gamma$  production by tg4 T cells in CRP-MBP livers compared with tg4 cells from control livers (Figure 3D). Accordingly, we observed a 6-fold increase in hepatic expression of the IFN $\gamma$ -inducible chemokine (C-X-C motif) ligand (*Cxcl9*) in CRP-MBP mice (Figure 3E) and increased expression of the C-X-C motif chemokine receptor(*Cxcr3*), as assessed by quantitative polymerase chain reaction (qPCR) using RNA from liver tissue (Figure 3F), and as confirmed by flow cytometry of MBP-specific CD4 T cells (Figure 3G). These findings suggested that the activation of MBP-specific T cells in CRP-MBP livers induced their redirection from the hepatic sinusoids into the parenchyma by IFN $\gamma$ - and CXCR3/CXCL9-dependent endothelial transmigration. Moreover, we observed up-regulation of several other recruitment molecules that are known to facilitate lymphocytic transmigration into the hepatic parenchyma (Figure 3H),<sup>25</sup> including *Aoc3* (Vascular adhesion protein (VAP)-1),<sup>26</sup> *Cxcr6*,<sup>27</sup> *Itga4*,<sup>28</sup> and *Madcam1*,<sup>28</sup> confirming the notion that MBP-specific T cells were redirected from the circulation into the liver.

### *Autoreactive T-Cell Accumulation in CRP-MBP Livers Is Dependent on the IFN $\gamma$ -CXCL9-CXCR3 Axis*

To test the functional role of IFN $\gamma$ -mediated tg4 T-cell recruitment into the liver of CRP-MBP mice, we repeated these experiments with additional administration of an inhibitory antibody to IFN $\gamma$  twice a week. On day 6 after cell transfer, hepatic expression of *Cxcl9* and *Cxcr3* was reduced



significantly in anti-IFN $\gamma$ -treated CRP-MBP mice to expression levels similar to those in control mice (Figure 4A and B). As a consequence of the inhibited IFN $\gamma$ -CXCL9-CXCR3 axis, we found significantly reduced numbers of MBP-specific T cells accumulating in the livers of CRP-MBP mice (Figure 4C). Liver histology confirmed a substantial reduction of periportal infiltration after IFN $\gamma$  inhibition (Figure 4D). Having thus shown that the recruitment of autoreactive effector T cells into the liver of tolerant CRP-MBP mice was IFN $\gamma$  dependent, we next tested whether inhibition of IFN $\gamma$  could break hepatic tolerance and induce autoimmune pathology in the CNS. To that end, we analyzed the occurrence of EAE symptoms in CRP-MBP mice and littermate controls that were treated with an IFN $\gamma$ -inhibiting antibody or isotype control. Indeed, IFN $\gamma$  inhibition induced mild symptoms of EAE in CRP-MBP mice compared with isotype control-treated mice (Figure 4E), confirming the functional role of IFN $\gamma$  in hepatic CD4 T-cell tolerance induction. However, blockade of IFN $\gamma$  alone was not sufficient to fully abrogate liver-induced tolerance and suppression of EAE.

### Up-Regulation of Immune Checkpoint Molecules by Autoreactive T Cells Facilitates Hepatic Tolerance in MBP-Transgenic Mice

Next, we investigated the phenotype of liver-infiltrating MBP-specific tg4 cells in CRP-MBP mice to understand the tolerogenic reprogramming of autoreactive CD4 T cells beyond induction of Tregs<sup>6</sup> or Tr1 cells (Figure 2). Interestingly, we found that the expression of several immune checkpoint genes, including *Ctla4*, *Lag3*, *Pdcd1* (encoding for programmed cell death 1 [PD-1]), *Tigit*, and *Havcr2* (encoding for T-cell immunoglobulin and mucin domain-containing protein 3 [TIM3]) was strongly and significantly up-regulated in the liver (Figure 5A). To confirm this finding on a protein level directly in the autoreactive T cells recognizing hepatic MBP, we analyzed the transferred tg4 T cells in the livers of CRP-MBP mice or WT mice by flow cytometry. Indeed, CTLA-4, LAG3, PD-1, T-cell immunoreceptor with Ig and immunoreceptor tyrosine-based inhibitory motif (ITIM) domains (TIGIT), and TIM3 were up-regulated significantly in the transferred tg4 T cells retrieved from the livers of CRP-MBP mice, as compared with those retrieved from littermate controls (Figure 5B and C).

Using t-distributed stochastic neighbor embedding, we studied the co-expression of these immune checkpoints on transferred MBP-specific T cells in CRP-MBP mice and

littermate controls (Figure 5D). We found immune checkpoints often co-expressed and identified a population of checkpoint-rich cells<sup>29</sup> that was 7 times more abundant in CRP-MBP mice compared with littermate controls (17.3% vs 2.4%). These findings indicated that autoreactive tg4 T cells, upon recognition of MBP in MBP-expressing, but not in WT, livers, up-regulated various immune checkpoint molecules considered to desensitize T cells.

### IFN $\gamma$ and CTLA-4 Are Essential for the Maintenance of Hepatic Tolerance in MBP-Transgenic Mice

We hypothesized that functional impairment of immune checkpoint molecules might be required to break hepatic tolerance in CRP-MBP mice. Given the essential role of CTLA-4 as a key inhibitor of autoimmunity,<sup>30</sup> we treated CRP-MBP mice with anti-CTLA-4 antibody after immunization to MBP. However, whereas anti-CTLA-4 treatment alone did not induce clinical EAE, combined administration of anti-CTLA-4 and anti-IFN $\gamma$  led to a breakdown of hepatic tolerance resulting in clinical EAE in CRP-MBP mice comparable with isotype-treated littermate controls (Figure 6A and B). Thus, antigen-specific CD4 T-cell tolerance induction in CRP-MBP mice resulted from IFN $\gamma$ -dependent redirection of circulating effector T cells into the liver parenchyma, and local induction of multiple immune checkpoints, notably CTLA-4, in autoreactive CD4 T cells.

## Discussion

Tregs are important mediators of immune tolerance and their role in liver-induced immune tolerance was shown in the CRP-MBP model in which transfer of CD4+CD25+ T cells protected mice from overt disease.<sup>6</sup> Moreover, protection from autoimmune disease after nanoparticle-mediated autoantigen peptide transfer to liver sinusoidal endothelial cells was critically dependent on CD25+FOXP3+ Tregs.<sup>7</sup> Yet, here we show that impairment of FOXP3+CD25+ Tregs did not cause a loss of established tolerance to MBP in CRP-MBP mice (Figure 1), indicating that Treg-independent mechanisms safeguarded liver-induced immune tolerance in this model. Interestingly, Treg-independent tolerance mechanisms also were found in other mouse models, such as hemolytic anemia,<sup>31</sup> or prostate cancer, in which Treg impairment did not break antigen-specific peripheral T-cell tolerance.<sup>32</sup> Furthermore, in a mouse model of autoimmune hepatitis, loss of Tregs alone was not sufficient for disease precipitation, which

**Figure 2.** (See previous page). Tr1-derived IL10 is not required for maintenance of hepatic tolerance in CRP-MBP mice. CRP-MBP mice or littermate controls (WT) were immunized to MBP and replenished with MBP-specific CD4 T cells 1 day later. (A) LAG3 and CD49b expression in transferred tg4 T cells retrieved from liver of WT (left panel) or CRP-MBP mice (right panel) 7 days after immunization. (B and C) Hepatic induction of MBP-specific IL10+LAG3+CD49b+ Tr1 cells. (D) EAE development in WT or CRP-MBP mice receiving isotype or IL10R antibody. (E) EAE course in triple-transgenic tg4 CD4dnlIL10R $\alpha$  mice with impaired IL10-receptor signaling, with or without additional application of Treg-depleting PC61.5.3 antibody, in comparison with tg4 control mice. Data are shown as means  $\pm$  SD, n = 4–6 per group. Data of 1 independent experiment of 2 independent experiments are shown. Statistical analysis was performed using the Mann-Whitney U test for comparison of 2 groups; for multiple comparisons the Kruskal-Wallis test with the Dunn multiple comparison test were used. \*P < .05, \*\*P < .01. APC, Allophycocyanin; PE, Phycoerythrin; RFP, Red Fluorescent Protein; spec., specific.

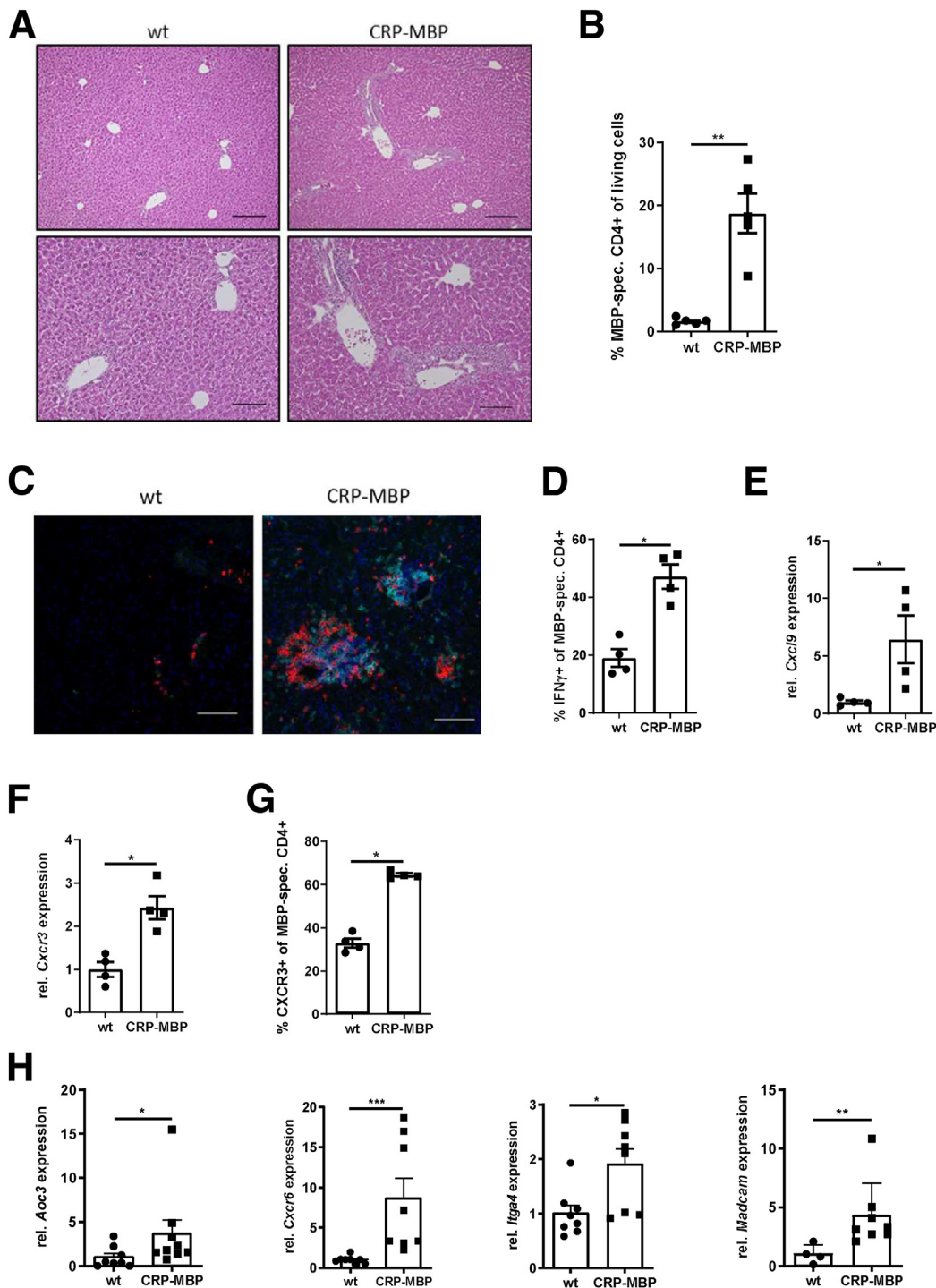


**Figure 3. MBP-specific T cells accumulate in livers of CRP-MBP mice.** CRP-MBP mice or littermate controls (WT) were immunized to MBP and replenished with MBP-specific CD4 T cells 1 day later. (A and B) On day 7 after immunization, lymphocytic infiltration was visualized in H&E staining of the liver. Scale bar: 200  $\mu$ m (upper panels); 100  $\mu$ m (lower panels). Hepatic accumulation of transferred MBP-specific CD4 T cells in the liver was determined by flow cytometry. (C) Accumulation of MBP-specific CD4<sup>+</sup> T cells (red) and endogenous CD45.1<sup>+</sup> immune cells (light blue) 6 days after adoptive transfer. Representative images of WT (left) and CRP-MBP livers (right) are shown, respectively. Scale bar: 100  $\mu$ m. (D) IFN $\gamma$  expression in tg4 T cells retrieved from livers of CRP-MBP or WT mice. (E and F) Cxcl9 and Cxcr3 expression in whole liver tissue. (G) Surface expression of CXCR3 on MBP-specific T cells in the liver. (H) Gene expression of recruitment molecules Aoc3 (VAP-1), Cxcr6, Itga4, and Madcam1 in whole liver tissue. Data are depicted as means  $\pm$  SD. n = 4–8. Data from 1 representative experiment out of multiple independent experiments are shown. Statistical analysis was performed using the Mann-Whitney U test. \* $P$  < .05, \*\* $P$  < .01, \*\*\* $P$  < .001. rel., relative; spec., specific.

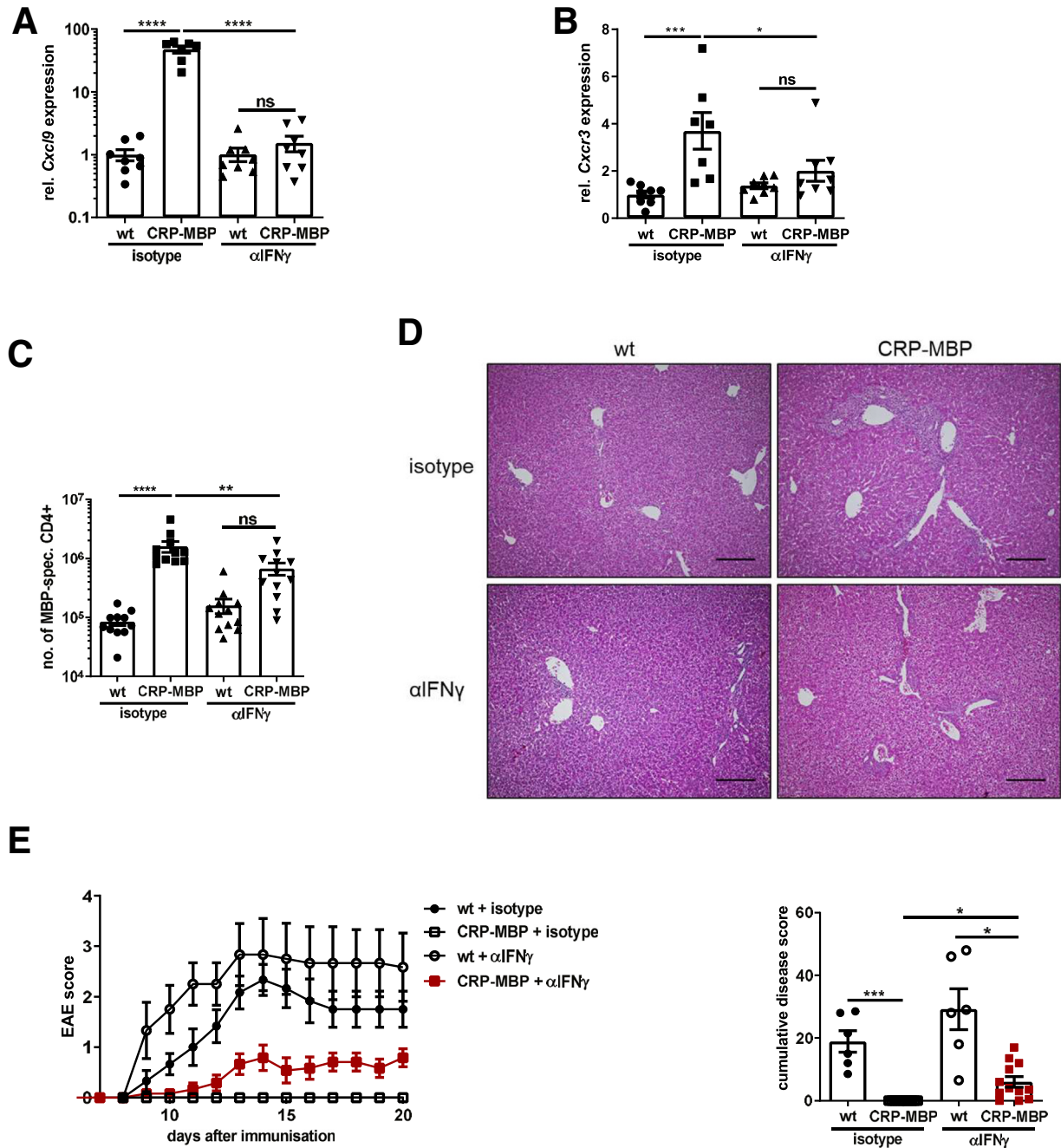


**Figure 4. Autoreactive T-cell accumulation in CRP-MBP livers is dependent on the IFN $\gamma$ -CXCL9-CXCR3 axis.** MBP-specific CD4 T cells from tg4 mice were transferred into immunized CRP-MBP mice or littermate controls (WT). On day 3 and day 6, mice were injected with 300  $\mu$ g anti-IFN $\gamma$  or isotype antibody. On day 7 after immunization, hepatic expression of (A) Cxcl9 and (B) Cxcr3 was determined. (C) Quantification of the absolute number of liver-infiltrating MBP-specific T cells and (D) H&E staining of hepatic infiltrates. Scale bar: 200  $\mu$ m. (E) CRP-MBP or littermate control mice were immunized to MBP and replenished with MBP-specific CD4 T cells 1 day later. On days 3, 6, 9, and 12 after immunization, mice were injected with 300  $\mu$ g anti-IFN $\gamma$  or isotype control antibodies. The EAE score was monitored for 20 days and the cumulative disease score was calculated. Data are depicted as means  $\pm$  SD.  $n = 6-12$ . Pooled data from 2 independent experiments are shown. Statistical analysis was performed using the Kruskal-Wallis test with the Dunn multiple comparison test. \* $P < .05$ , \*\* $P < .01$ , \*\*\* $P < .001$ , and \*\*\*\* $P < .0001$ . rel., relative; spec., specific.

required additional knockout of the checkpoint molecule PD-1.<sup>33</sup> We observed hepatic induction of MBP-specific LAG3+CD49b+IL10+ Tr1 cells in our model, and a regulatory role of Tr1 cells in the liver has been described before.<sup>17,18</sup> Because it is difficult to deplete Tr1 cells in vivo,

we tested whether their functional impairment by blockade of IL10 signaling would affect hepatic tolerance. IL10 is considered the major regulatory mechanism of Tr1 cells,<sup>16</sup> yet a proinflammatory role of CD4+ T-cell-derived IL10 in CNS inflammation also recently was described.<sup>34</sup> Either



way, blockade of IL10 signaling did not precipitate autoimmune disease in these mice (Figure 2), indicating that IL10 was irrelevant for tolerance to MBP. Thus, maintenance of peripheral immune tolerance cannot be easily reduced to single-tolerance mechanisms, such as Treg- or IL10-mediated suppression of autoreactive cells, but seems to rely on additional and complementary mechanisms.

Indeed, Treg impairment seemed to be compensated for by the IFN $\gamma$ -dependent hepatic accumulation and desensitization of autoreactive CD4 T cells in autoantigen-expressing livers of tolerant CRP-MBP mice (Figures 3 and 4). It previously was shown that after immunization of mice to MBP, activated MBP-specific T cells showed a complex migration pattern leading from draining lymph nodes to the spleen, and from there to the circulation, followed by their entry into the CNS.<sup>35</sup> In our model, while on their way to the CNS, recognition of MBP in the liver induced the redirection of the activated MBP-specific T cells into the liver mediated through an IFN $\gamma$ -CXCL9-CXCR3 axis. Intriguingly, blockade of IFN $\gamma$ , which was associated with reduced migration of MBP-specific T cells into the liver, partially impaired hepatic tolerance induction and induced mild symptoms of EAE in CRP-MBP mice (Figure 4E). Interestingly, in a mouse model of hepatitis B virus (HBV) infection, susceptibility to chronic HBV infection likewise was dependent on the redirection of circulating antiviral CD4 T cells into the liver via the IFN $\gamma$ -CXCL9-CXCR3 axis; yet tolerance to HBV has been linked to subsequent CD4 T-cell apoptosis,<sup>36</sup> which was not a dominant T-cell response in our model. The marked up-regulation of several immune checkpoint molecules, including CTLA-4, LAG-3, PD-1, TIM3, and TIGIT (Figure 5) by autoreactive CD4 T cells in MBP-expressing livers indicated acquisition of a tolerant phenotype.<sup>37,38</sup> Note that sole inhibition of IFN $\gamma$  or CTLA-4 failed to completely break hepatic tolerance in CRP-MBP mice, whereas combined inhibition of IFN $\gamma$  and CTLA-4 completely abolished MBP-specific tolerance and resistance to EAE (Figure 6B). These findings highlight the crucial synergistic effects of IFN $\gamma$  and CTLA-4 in hepatic induction of antigen-specific CD4 T-cell tolerance *in vivo*. In this study, we could not evaluate whether one or several checkpoint molecules other than CTLA-4 would be of similar relevance for hepatic T-cell tolerance. Although different checkpoint molecules have distinct functions, it is conceivable that their inhibition would produce similar effects as inhibition of CTLA-4 because they redundantly mediate tolerance.<sup>30</sup> It recently was reported that type I interferons can drive up-regulation of immune checkpoints through IL10 signaling<sup>39</sup>; however, because blockade of IL10 signals in our model did not break tolerance, one should consider additional pathways redundant to IL10.

In summary, we show that systemic CD4 T-cell tolerance induction to hepatic antigen depends on IFN $\gamma$ -CXCL9-CXCR3-mediated accumulation of antigen-specific T cells in the liver, and subsequent up-regulation of multiple immune checkpoint molecules, most notably CTLA-4. These findings also might explain the observation that IFN $\gamma$  was found essential for spontaneous acceptance of liver allografts.<sup>40</sup> Of note, the combined activity of IFN $\gamma$  and immune checkpoint molecules not only seems to

explain liver-induced tolerance to alloantigens or autoantigens, but also might be a relevant mechanism preventing effective elimination of aberrant cells or pathogens, thereby promoting cancer or chronic infection. Indeed, the liver is distinctly permissive for primary and secondary tumors, and for chronic infections; these conditions often are marked by up-regulation of checkpoint molecules on T cells,<sup>10</sup> which usually are regarded as markers of T-cell exhaustion.<sup>41</sup> Although exhaustion is not well defined in CD4 T cells, it is clear that the phenotype of the desensitized autoreactive T cells described here is highly reminiscent of that of the T cells in liver cancer or chronic infection. Our study shows that hepatic tolerance can best be targeted by concomitant inhibition of IFN $\gamma$  and checkpoint molecules, such as CTLA-4, suggesting that such combined treatment also might be effective in liver cancer and chronic liver infections.

## Material and Methods

### Mice

For adoptive transfer of MBP-specific CD4 T cells from T-cell-receptor-transgenic tg4 mice,<sup>19</sup> CRP-MBP mice on a (C57BL/6J  $\times$  B10.PL) F1 background with hepatic MBP expression<sup>6</sup> or their nontransgenic littermates were used as recipients. As indicated, the tg4 T cells had additional mutations, such as a dnIL10R<sup>24</sup> (tg4 CD4dnIL10R $\alpha$  mice), or IL10 reporter activity<sup>22</sup> (tg4 IL10<sup>eGFP</sup> reporter mice). For discrimination of endogenous or transferred cells, donor mice were homozygous for CD45.2; congenic recipient mice were heterozygous for CD45.1 and CD45.2. All mice were bred and kept in the animal facility of the University Medical Center Hamburg-Eppendorf under specific pathogen-free conditions with 12-hour light/dark cycles and access to standard chow diet (1318 rodent diet; Altromin) and water *ad libitum*. Both sexes were used in age- and sex-matched groups for experiments because we did not observe any sex-related differences in our analyses. All animal experiments were approved by the review board of the State of Hamburg, Germany, and comply with the Animal Research: Reporting of In Vivo Experiments (ARRIVE) guidelines (<https://www.nc3rs.org.uk/arrive-guidelines>).

### Inflammatory Priming of Autoreactive CD4 T Cells *In Vivo*

Age- and sex-matched mice were injected subcutaneously at the base of the tail with 200  $\mu$ g MBP Ac1-9 peptide<sup>6</sup> in 0.1 mL of an emulsion of PBS and complete Freund's adjuvant containing 4 mg/mL heat-killed *Mycobacterium tuberculosis*, strain H37RA (Difco). On the day of immunization and 2 days later, 200 ng pertussis toxin (Sigma-Aldrich) was injected intraperitoneally in 0.25 mL PBS. The development of EAE was monitored daily for up to 30 days after immunization. The severity of EAE was scored as follows: 1, flaccid tail; 2, partial hindlimb paralysis; 3, complete hindlimb paralysis; 4, forelimb and hindlimb paralysis; and 5, moribund. Treatment with anti-IFN $\gamma$  antibody leads to atypical EAE symptoms in some mice. These were scored as follows: 0, no clinical signs; 1, slight head tilt; 2, severe head tilt; 3, slight axial rotation/staggered walking; 4, severe axial

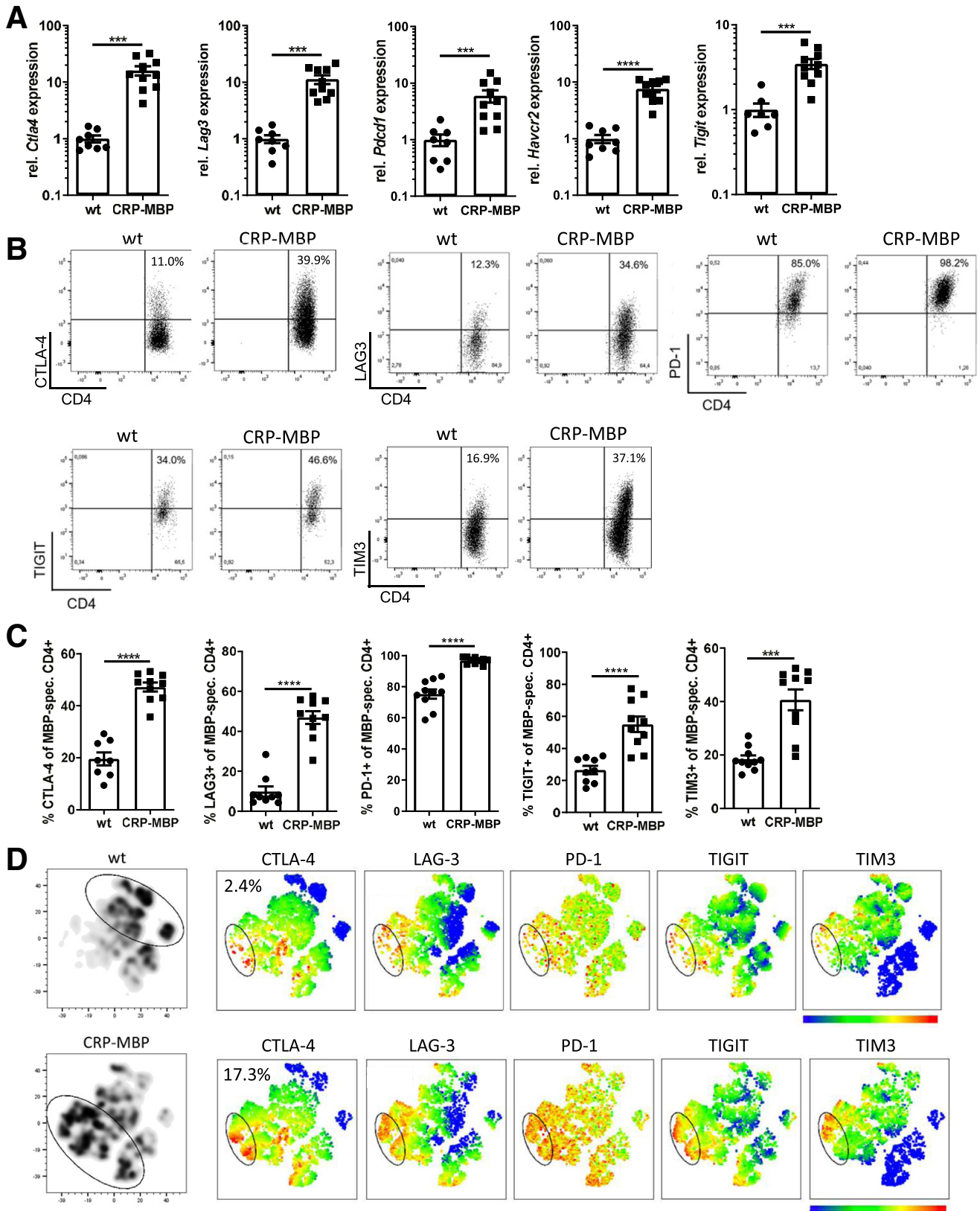


**Figure 5. MBP-specific T cells up-regulate co-inhibitory receptors in livers of CRP-MBP mice.** CRP-MBP mice or littermate controls (WT) were immunized to MBP and replenished with MBP-specific CD4 T cells 1 day later. (A) On day 7 after immunization, co-inhibitory-receptor expression was analyzed in whole liver tissue. (B–D) Transferred MBP-specific CD4 T cells were retrieved from the liver and analyzed for the expression of CTLA-4, LAG3, PD-1, TIM3, TIGIT, and CTLA-4 in (B) representative FACS plots and (C) quantitative analysis. (D) t-distributed stochastic neighbor embedding (tSNE) analysis was performed on MBP-specific T cells based on expression of LAG3, PD-1, TIM3, TIGIT, and CTLA-4. Data are depicted as means  $\pm$  SD. (A–C)  $n = 8$ –10, representing pooled data from 2 independent experiments. (D)  $n = 4$ , data from 1 representative experiment out of 4 independent experiments are shown. Statistical analysis was performed using the Mann-Whitney  $U$  test. \*\*\* $P < .001$ , \*\*\*\* $P < .0001$ . rel., relative; spec., specific.

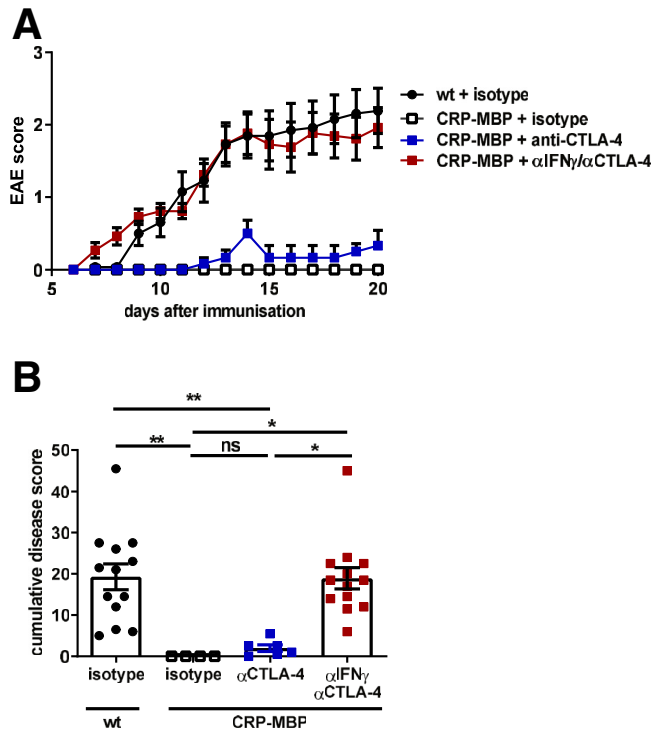


**Figure 6. IFN $\gamma$  and CTLA-4 drive liver-induced systemic immune tolerance in MBP-transgenic mice.** (A and B) CRP-MBP or littermate control mice were immunized to MBP and replenished with MBP-specific CD4 T cells 1 day later. On days 3, 6, 9, and 12 after immunization, mice were injected with 300  $\mu$ g anti-CTLA-4, a mixture of anti-IFN $\gamma$  and anti-CTLA-4 or isotype control antibodies. The EAE score was monitored for 20 days and the cumulative disease score was calculated. Data are depicted as means  $\pm$  SD.  $n = 4$ –13. Pooled data from 2 independent experiments are shown. (B) Statistical analysis was performed using the Kruskal–Wallis test with the Dunn multiple comparison test. \* $P < .05$ , \*\* $P < .01$ .

rotation/spinning; and 5, moribund.<sup>42</sup> Mice were killed when reaching a score between 3 and 4 according to defined termination criteria. For the cumulative disease score, daily clinical scores of each mouse were summarized over the EAE observation period.

### In Vivo Antibody Blockade

For in vivo depletion of regulatory T cells, 500  $\mu$ g anti-CD25 antibody (PC61.5.3; BioXCell) was administered intraperitoneally in 0.2 mL PBS twice a week.<sup>43</sup> For in vivo impairment of IFN $\gamma$  (XMG1.2; BioXCell/BioLegend) and CTLA-4 (UC10-4F10-11; BioXCell), 300  $\mu$ g antibody was administered intraperitoneally in 0.2 mL PBS twice a week. Rat IgG1 anti-horseradish peroxidase was used in equal concentration and volume as isotype control for anti-CD25 and anti-IFN $\gamma$ . Armenian hamster IgG was used as isotype control for anti-CTLA-4. For in vivo impairment of IL10 signaling, 150  $\mu$ g inhibitory antibody to the IL10 receptor<sup>23</sup> was administered intraperitoneally 1 day before immunization with MBP peptide and once a week afterward.

### Isolation of Liver and Spleen Leukocytes

For isolation of liver nonparenchymal cells (NPCs), livers were perfused with PBS via the hepatic portal vein and mechanically dissected to generate single-cell suspensions. Hepatocytes and debris were sedimented and NPCs were recovered via centrifugation over a 21% Optiprep gradient (Sigma-Aldrich).<sup>44</sup> For adoptive transfer experiments, splenic CD4 T cells were sorted by magnetic-activated cell sorting from single-cell suspensions according to the manufacturer's protocol (Miltenyi Biotec). Erythrocytes were lysed using red blood cell lysis buffer (BioLegend).

### Adoptive Transfer of Autoreactive CD4 T Cells

For adoptive T-cell transfer,  $5 \times 10^6$  MBP-specific CD45.1- CD45.2+ CD4 T cells from spleens of tg4 mice, tg4 IL10<sup>eGFP</sup> reporter mice, or tg4 CD4dnIL10R $\alpha$  mice cells were injected into the tail vein of CD45.1+ CD45.2+ recipient mice. On day 6 after transfer, the transferred CD45.1- CD45.2+ autoreactive T cells were retrieved from livers and spleens of recipient mice and analyzed by flow cytometry.

### Liver Histology

Formalin-fixed paraffin liver sections were stained with H&E to visualize lymphocytic infiltration. Alternatively, histologic sections of freshly frozen livers were stained with fluorochrome-labeled antibodies against CD4 and CD45.1 (BioLegend), and Hoechst 33258 nuclear stain (Sigma-Aldrich). Pictures were taken with a BZ-9000 microscope (Keyence).

### Flow Cytometry

Fluorochrome-labeled antibodies to CD4, CD25, CD49b, CD45.1, TIM3 and IFN $\gamma$  were purchased from BioLegend, antibodies to LAG3 and FOXP3 from eBioscience, and antibodies to CTLA-4 and TIGIT from BD Biosciences. FOXP3, IFN $\gamma$ , and CTLA-4 were stained using the FOXP3/Transcription Factor Staining Buffer Set (eBioscience). For exclusion of dead cells, all samples were stained with Pacific Orange-NHS (Life Technologies). To detect cytokine production, NPCs or splenocytes were restimulated with phorbol myristate acetate (100 ng/mL) and ionomycin (1  $\mu$ g/mL) in the presence of Golgi Plug (1  $\mu$ g/mL; BD Biosciences) for 4 hours before staining. Samples were acquired on an LSR II flow cytometer (BD Biosciences) and analyzed using FlowJo (FlowJo, LLC).

### RNA Isolation, Complementary DNA Synthesis, and Real-Time qPCR

Total liver RNA was prepared with the NucleoSpin RNA Kit (Macherey-Nagel) according to the manufacturer's instructions. RNA was reverse-transcribed to complementary DNA with the High-Capacity Complementary DNA Reverse-Transcription Kit (Thermo Fisher Scientific). To determine the relative expression level of each gene of interest, qPCR was performed with TaqMan probes and the KAPA Probe Fast qPCR Master Mix (2 $\times$ ) Kit (Roche). RNA expression of

target genes (*Ctla4*: Mm00486849\_m1; *Cxcl9*: Mm00434946\_m1; *Cxcr3*: Mm99999054\_s1; *Havcr2*: Mm00454540\_m1; *Lag3*: Mm00493071\_01; *Pdcd1*: Mm01285676\_m1; *Tigit*: Mm03807522\_m1; *Aoc3*: Mm00839624\_m1; *Cxcr6*: Mm02620517\_s1, *Itga4*: Mm01277951\_m1; and *Madcam1*: Mm00522088\_m1) was determined with probes from Thermo Fisher Scientific relative to the expression of hypoxanthine-guanine phosphoribosyltransferase (*Hprt*) (Mm00446968\_m1).

### Statistics

Statistical analyses between 2 data sets were conducted with the Mann–Whitney test. For comparisons of multiple groups, the Kruskal–Wallis test with the Dunn multiple comparisons test was performed. A *P* value less than .05 was considered statistically significant.

All authors had access to the study data and reviewed and approved the final manuscript.

### References

- Racanelli V, Rehermann B. The liver as an immunological organ. *Hepatology* 2006;43:S54–S62.
- Thomson AW, Knolle PA. Antigen-presenting cell function in the tolerogenic liver environment. *Nat Rev Immunol* 2010;10:753–766.
- Cantor HM, Dumont AE. Hepatic suppression of sensitization to antigen absorbed into the portal system. *Nature* 1967;215:744–745.
- Calne RY, Sells RA, Pena JR, et al. Induction of immunological tolerance by porcine liver allografts. *Nature* 1969;223:472–476.
- Sriwatanawongsa V, Davies HFS, Calne RY. The essential roles of parenchymal tissues and passenger leukocytes in the tolerance induced by liver grafting in rats. *Nat Med* 1995;1:428–432.
- Lüth S, Huber S, Schramm C, et al. Ectopic expression of neural autoantigen in mouse liver suppresses experimental autoimmune neuroinflammation by inducing antigen-specific Tregs. *J Clin Invest* 2008;118:3403–3410.
- Carambia A, Freund B, Schwinge D, et al. Nanoparticle-based autoantigen delivery to Treg-inducing liver sinusoidal endothelial cells enables control of autoimmunity in mice. *J Hepatol* 2015;62:1349–1356.
- Heymann F, Peusquens J, Ludwig-Portugall I, et al. Liver inflammation abrogates immunological tolerance induced by Kupffer cells. *Hepatology* 2015;62:279–291.
- Carambia A, Gottwick C, Schwinge D, et al. Nanoparticle-mediated targeting of autoantigen peptide to cross-presenting liver sinusoidal endothelial cells protects from CD8 T-cell-driven autoimmune cholangitis. *Immunology* 2021;162:452–463.
- Zheng M, Tian Z. Liver-mediated adaptive immune tolerance. *Front Immunol* 2019;10:2525.
- Lee JC, Mehdizadeh S, Smith J, et al. Regulatory T cell control of systemic immunity and immunotherapy response in liver metastasis. *Sci Immunol* 2020;5:eaba0759.
- Carambia A, Frenzel C, Bruns OT, et al. Inhibition of inflammatory CD4 T cell activity by murine liver sinusoidal endothelial cells. *J Hepatol* 2013;58:112–118.
- Diehl L, Schurich A, Grochtmann R, et al. Tolerogenic maturation of liver sinusoidal endothelial cells promotes B7-homolog 1-dependent CD8+ T cell tolerance. *Hepatology* 2008;47:296–305.
- Limmer A, Arnold B, Knolle PA. Efficient presentation of exogenous antigen by liver endothelial cells to CD8+ T cells results in antigen-specific T-cell tolerance. *Nat Med* 2000;6:1348–1354.
- Carambia A, Freund B, Schwinge D, et al. TGF- $\beta$ -dependent induction of CD4+CD25+FOXP3+ Tregs by liver sinusoidal endothelial cells. *J Hepatol* 2014;61:594–599.
- Roncarolo MG, Gregori S, Bacchetta R, et al. Tr1 cells and the counter-regulation of immunity: natural mechanisms and therapeutic applications. *Curr Top Microbiol Immunol* 2014;380:39–68.
- Xu L, Yin W, Sun R, et al. Liver type I regulatory T cells suppress germinal center formation in HBV-tolerant mice. *Proc Natl Acad Sci U S A* 2013;110:16993–16998.
- Ye F, Yan S, Xu L, et al. Tr1 regulatory T cells induced by ConA pretreatment prevent mice from ConA-induced hepatitis. *Immunol Lett* 2009;122:198–207.
- Liu GY, Fairchild PJ, Smith RM, et al. Low avidity recognition of self-antigen by T cells permits escape from central tolerance. *Immunity* 1995;3:407–415.
- Gagliani N, Magnani CF, Huber S, et al. Coexpression of CD49b and LAG-3 identifies human and mouse T regulatory type 1 cells. *Nat Med* 2013;19:739–746.
- Brockmann L, Soukou S, Steglich B, et al. Molecular and functional heterogeneity of IL-10-producing CD4+ T cells. *Nat Commun* 2018;9:5457.
- Brockmann L, Gagliani N, Steglich B, et al. IL-10 receptor signaling is essential for Tr1 cell function in vivo. *J Immunol* 2017;198:1130–1141.
- Lin CC, Bradstreet TR, Schwarzkopf EA, et al. Bhlhe40 controls cytokine production by T cells and is essential for pathogenicity in autoimmune neuroinflammation. *Nat Commun* 2014;5:3551.
- Kamanaka M, Huber S, Zenewicz LA, et al. Memory/effector (CD45RB(lo)) CD4 T cells are controlled directly by IL-10 and cause IL-22-dependent intestinal pathology. *J Exp Med* 2011;208:1027–1040.
- Shetty S, Lalor PF, Adams DH. Liver sinusoidal endothelial cells - gatekeepers of hepatic immunity. *Nat Rev Gastroenterol Hepatol* 2018;15:555–567.
- Lalor PF, Edwards S, McNab G, et al. Vascular adhesion protein-1 mediates adhesion and transmigration of lymphocytes on human hepatic endothelial cells. *J Immunol* 2002;169:983–992.
- Heydtmann M, Lalor PF, Eksteen JA, et al. CXC chemokine ligand 16 promotes integrin-mediated adhesion of liver-infiltrating lymphocytes to cholangiocytes and hepatocytes within the inflamed human liver. *J Immunol* 2005;174:1055–1062.
- Grant AJ, Lalor PF, Hübscher SG, et al. MAdCAM-1 expressed in chronic inflammatory liver disease supports mucosal lymphocyte adhesion to hepatic endothelium

- (MAdCAM-1 in chronic inflammatory liver disease). *Hepatology* 2001;33:1065–1072.
29. Chihara N, Madi A, Kondo T, et al. Induction and transcriptional regulation of the co-inhibitory gene module in T cells. *Nature* 2018;558:454–459.
  30. Burke KP, Patterson DG, Liang D, et al. Immune checkpoint receptors in autoimmunity. *Curr Opin Immunol* 2023;80:102283.
  31. Richards AL, Kapp LM, Wang X, et al. Regulatory T cells are dispensable for tolerance to RBC antigens. *Front Immunol* 2016;7:348.
  32. Degl'Innocenti E, Grioni M, Capuano G, et al. Peripheral T-cell tolerance associated with prostate cancer is independent from CD4+CD25+ regulatory T cells. *Cancer Res* 2008;68:292–300.
  33. Kido M, Watanabe N, Okazaki T, et al. Fatal autoimmune hepatitis induced by concurrent loss of naturally arising regulatory T cells and PD-1-mediated signaling. *Gastroenterology* 2008;135:1333–1343.
  34. Yogev N, Bedke T, Kobayashi Y, et al. CD4+ T-cell-derived IL-10 promotes CNS inflammation in mice by sustaining effector T cell survival. *Cell Rep* 2022;38:110565.
  35. Flügel A, Berkowicz T, Ritter T, et al. Migratory activity and functional changes of green fluorescent effector cells before and during experimental autoimmune encephalomyelitis. *Immunity* 2001;14:547–560.
  36. Zeng Z, Li L, Chen Y, et al. Interferon-gamma facilitates hepatic antiviral T cell retention for the maintenance of liver-induced systemic tolerance. *J Exp Med* 2016;213:1079–1093.
  37. Anderson AC, Joller N, Kuchroo VK. Lag-3, Tim-3, and TIGIT: co-inhibitory receptors with specialized functions in immune regulation. *Immunity* 2016;44:989–1004.
  38. Nguyen LT, Ohashi PS. Clinical blockade of PD1 and LAG3–potential mechanisms of action. *Nat Rev Immunol* 2015;15:45–56.
  39. Hackstein CP, Spitzer J, Symeonidis K, et al. Interferon-induced IL-10 drives systemic T-cell dysfunction during chronic liver injury. *J Hepatol* 2023;79:150–166.
  40. Mele TS, Kneteman NM, Zhu LF, et al. IFN-gamma is an absolute requirement for spontaneous acceptance of liver allografts. *Am J Transplant* 2003 Aug;3(8):942–951.
  41. Blank CU, Haining WN, Held W, et al. Defining 'T cell exhaustion'. *Nat Rev Immunol* 2019;19:665–674.
  42. Naves R, Singh SP, Cashman KS, et al. The interdependent, overlapping, and differential roles of type I and II IFNs in the pathogenesis of experimental autoimmune encephalomyelitis. *J Immunol* 2013;191:2967–2977.
  43. Sakaguchi S, Sakaguchi N, Asano M, et al. Immunologic self-tolerance maintained by activated T cells expressing IL-2 receptor alpha-chains (CD25). Breakdown of a single mechanism of self-tolerance causes various autoimmune diseases. *J Immunol* 1995;155:1151–1164.
  44. Schwinge D, Carambia A, Quaas A, et al. Testosterone suppresses hepatic inflammation by the downregulation of IL-17, CXCL-9, and CXCL-10 in a mouse model of experimental acute cholangitis. *J Immunol* 2015;194:2522–2530.

---

Received May 12, 2023. Accepted September 12, 2023.

#### Correspondence

Address correspondence to: Johannes Herkel, PhD, or Antonella Carambia, PhD, Department of Medicine I, University Medical Centre Hamburg-Eppendorf, Martinstraße 52, 20246 Hamburg, Germany. e-mail: jherkel@uke.de or a.carambia@uke.de.

#### Acknowledgments

The authors are grateful for excellent technical assistance by Marko Hilken, Sabrina Kreß, Angelika Schmidt, and Jennifer Wigger.

#### CRedit Authorship Contributions

Daria Krzikalla (Conceptualization: Equal; Formal analysis: Lead; Investigation: Lead; Methodology: Lead; Software: Lead; Validation: Lead; Visualization: Lead; Writing – original draft: Equal)

Alena Laschtowitz (Formal analysis: Equal; Investigation: Equal; Writing – review & editing: Supporting)

Lisa Leyboldt (Formal analysis: Equal; Investigation: Equal; Writing – review & editing: Supporting)

Cornelia Gottwick (Investigation: Supporting; Writing – review & editing: Supporting)

Pia Averhoff (Investigation: Supporting; Writing – review & editing: Supporting)

Sören Weidemann (Methodology: Supporting; Writing – review & editing: Supporting)

Ansgar W. Lohse (Conceptualization: Supporting; Funding acquisition: Supporting; Writing – review & editing: Supporting)

Samuel Huber (Methodology: Supporting; Resources: Supporting; Writing – review & editing: Supporting)

Christoph Schramm (Conceptualization: Supporting; Writing – review & editing: Supporting)

Dorothee Schwinge (Conceptualization: Supporting; Methodology: Supporting; Writing – review & editing: Supporting)

Johannes Herkel (Conceptualization: Lead; Data curation: Lead; Formal analysis: Equal; Funding acquisition: Lead; Investigation: Supporting; Methodology: Equal; Project administration: Equal; Resources: Lead; Supervision: Lead; Writing – original draft: Lead)

Antonella Carambia (Conceptualization: Lead; Data curation: Equal; Formal analysis: Equal; Investigation: Supporting; Methodology: Lead; Supervision: Lead; Writing – original draft: Lead)

Present affiliation of D.K.: Topas Therapeutics GmbH, Hamburg, Germany.

#### Conflicts of interest

The authors disclose no conflicts.

#### Funding

This study was supported by the Deutsche Forschungsgemeinschaft, CRC 841. Also supported by the Open Access Publication Fund of the University Medical Center Hamburg-Eppendorf and Deutsche Forschungsgemeinschaft.

#### Data Availability

Data and analytic methods will be made available to other researchers upon request.